Radiocarbon Dating Comparée of Hyksos-Related Phases at Ashkelon and Tell el-Dab'a

Bruins, Hendrik J.; van der Plicht, Johannes

Published in:
The Enigma of the Hyksos Volume I

The Enigma of the Hyksos
Volume I

Contributions to the Archaeology of Egypt, Nubia and the Levant

CAENL

Edited by Manfred Bietak

Volume 9

2019
Harrassowitz Verlag · Wiesbaden

The Enigma of the Hyksos
Volume I

ASOR Conference Boston 2017 –
ICAANE Conference Munich 2018 – Collected Papers

Edited by
Manfred Bietak and Silvia Prell

2019
Harrassowitz Verlag · Wiesbaden

Cover illustration: redrawn by S. Prell after J. de Morgan, Fouilles à Dahchour: mars - juin 1894, Vienna 1895, figs. 137-140

This project has received funding from the European Research Council (ERC) under the European Union's Horizon 2020 research and innovation programme (grant agreement No 668640).

This publication has undergone the process of international peer review.

Bibliografische Information der Deutschen Nationalbibliothek
Die Deutsche Nationalbibliothek verzeichnet diese Publikation in der Deutschen Nationalbibliografie; detaillierte bibliografische Daten sind im Internet über http://dnb.dnb.de abrufbar.

Bibliographic information published by the Deutsche Nationalbibliothek
The Deutsche Nationalbibliothek lists this publication in the Deutsche Nationalbibliografie; detailed bibliographic data are available in the Internet at http://dnb.dnb.de

For further information about our publishing program consult our website http://www.harrassowitz-verlag.de

Printed on permanent/durable paper.
Typesetting and layout: u.ni medienservice, Hönze
Printing and binding: Hubert & Co., Göttingen
Printed in Germany

ISSN 2627-8022
ISBN 978-3-447-11332-8

Table of Contents

Radiocarbon Dating Comparée of Hyksos-Related Phases at Ashkelon and Tell el-Dabʿa

by Hendrik J. Bruins [1] and Johannes van der Plicht [2,3]

Dedication

This article is dedicated to the late Lawrence E. Stager (1943–2017), who was the founder and director of the Leon Levy Expedition to Ashkelon. These archaeological excavations, conducted from 1985 to 2016, yielded a host of important finds that advanced and will advance our understanding of the Hyksos period in the southern Levant and respective relations with Tell el-Dabʿa (Avaris). The workshop 'The Enigma of the Hyksos', held in Boston on 18 November 2017, was attended by Stager, about a month before his passing away on December 29.

Abstract

Radiocarbon dates of Ashkelon, the most important Middle Bronze Age site in Canaan along the southern Mediterranean coast, are compared with those of Tell el-Dabʿa, the Hyksos capital Avaris, focusing on archaeological phases associated with the Hyksos 15th Dynasty. The current calibration curve IntCal13 does not seem accurate for the period 1700–1500 BCE, in light of newly published dendrochronological datasets. Also, the issue of regional radiocarbon offsets is currently under renewed investigation. Therefore, we decided to present in this article a comparative analysis of the uncalibrated dates of Ashkelon and Tell el-Dabʿa. These basic measurements in conventional ^{14}C years BP remain valid, irrespective of the calibration curve. Thus, our article will not lose its value, as the new calibration curve IntCal19 will have been completed and released at some time during 2019. Anyhow, it does not make sense to use the present calibration curve IntCal13 for a study on the Hyksos period.

The earliest phases evaluated in this article are Ashkelon Grid 2, Phase 12 (Gate 3) and the related Tell el-Dabʿa Phases F and E/3, which precede the 15th Dynasty. The stratigraphic correlation of these late Middle Bronze (MB) IIA and early MB IIB phases at both sites, based on ceramics, is fully supported by our radiocarbon dating measurements of Ashkelon, in comparison to Tell el-Dabʿa. The next MB IIB strata, Ashkelon Grid 2, Phase 11 (Gate 4) and Tell el-Dabʿa Phases E/2, E/1 and D/3 (early to middle 15th Dynasty) also give analogous radiocarbon dates at both sites, again, fully backing the archaeological stratigraphic correlations based on pottery. The late 15th Dynasty is generally associated with the archaeological period MB IIC, related to Ashkelon Grid 2, Phase 10 and Tell el-Dabʿa Phases D/2 and D/1. But here the historical and archaeological correlations become more complex and disputed. Our current radiocarbon dating study of Ashkelon has not been able to obtain clear results for Grid 2, Phase 10. On the other hand, for Ashkelon Grid 50, Phase 11 we have a robust series of ten ^{14}C dates for Tomb Chamber 10. Comparing these uncalibrated dates with those of Tell el-Dabʿa and Ashkelon Grid 2, it becomes clear that Tomb Chamber 10 was in use during the 15th Dynasty and also during the early 18th Dynasty.

Introduction

During the writing of our manuscript in 2018, new articles with significant consequence for radiocarbon dating were published, which necessitated a different approach in our paper. Pearson et al.[4] measured the ^{14}C content in annual tree-rings of dendrochronologically dated wood for the period 1700–1500 BCE. This time frame covers the 15th Dynasty, the early 18th Dynasty and the Minoan Santorini eruption. Pearson et al. selected two tree species from different continents in the northern hemisphere: (1) bristlecone pine (*Pinus longaeva* D.K. Bailey) from the White Mountains of California (high elevation at a distance of c. 400 km east of the Pacific Ocean) and (2) oak (*Quercus* sp.) from County Kildare in Ireland (low elevation at a distance of c. 170 km east of the Atlantic Ocean).[5]

Their results show a distinct departure from the present calibration curve IntCal13[6] for the period 1680–1500,[7] resulting generally in somewhat later calibrated radiocarbon dates over this time trajectory. The new tree-ring ^{14}C dataset is interpreted by Pearson et al. to

1 Ben-Gurion University of the Negev, Professor Emeritus, Jacob Blaustein Institutes for Desert Research, Sede Boker Campus, Israel. hjbruins@bgu.ac.il.

2 University of Groningen, Professor Emeritus, Centre for Isotope Research, Groningen, The Netherlands.

3 University of Leiden, Faculty of Archaeology, Leiden, The Netherlands.

4 Pearson et al. 2018; Their annual radiocarbon curve indicates a 16th-century BCE date for the Thera eruption.

5 The distance from the oceans is here added by us, because ocean upwelling of 'old' CO_2 (Braziunas, Fung and Stuiver 1995) may cause the apparent age of trees to be older within a distance of c. 50 km from the coast in the northern hemisphere (Hagens 2014). Therefore, the trees investigated by Pearson et al. 2018, situated in areas with prevailing western winds, grew at a 'safe' distance away from the coast.

6 Reimer et al. 2013.

7 Pearson et al. 2018.

indicate a 16th-century date for the Minoan Santorini (Thera) eruption.[8] However, the possible lowering of calibrated radiocarbon dates, as indicated by the new dataset, is not sufficient to bridge the vexing gap of c. 100–120 years between conventional archaeo-historical dating and ^{14}C dating, both with regard to the Minoan eruption and Tell el-Dabʿa.[9] Nevertheless, we agree with Pearson et al. that "no definitive calibrated radiocarbon range for the Thera eruption is currently possible".[10] Likewise, calibrated radiocarbon dating of archaeological strata and Bayesian sequence analysis related to the 15th Dynasty and the early 18th Dynasty does not make sense at the moment.

In addition to this, a recent publication by Manning et al.[11], studying *Juniperus phoenicea* tree-rings from southern Jordan over the period 1610–1912 CE, measured a radiocarbon offset that fluctuates through time. Though the average value is c. 19 years, similar as found previously for different plants in Egypt,[12] the offset was found to be larger, 24 ± 5 radiocarbon years, during the period 1685–1762 CE and during 1818–1912 CE. However, other new annual tree-ring data indicate that the regional effect as published by Manning et al.[13] is probably only of the order of 0.1%, equivalent to 8 years BP.[14]

Preliminary discussions of results at the last Radiocarbon Conference in Trondheim, Norway (June 2018) suggest that the plateau around 1600 BCE in the present IntCal13 calibration curve[15] should probably be raised by about 20–25 years BP. At the time of writing of our manuscript, both aspects raised by Pearson et al. and Manning et al. are thoroughly being investigated by the radiocarbon community. A number of laboratories are performing many ^{14}C analyses in order to reach a consensus on revisions for the new calibration curve IntCal19, which is to be released in 2019.[16]

Concerning the most detailed radiocarbon dating of the Minoan Santorini eruption, based on growth rings in an olive wood branch found on Thera below the Plinian eruption phase,[17] the complicated growth of olive trees was raised as a possible problem.[18] In the resulting discussion,[19] it was suggested by Bruins and Van der Plicht[20] that "with regard to modern olive trees on Santorini and annual growth rings investigations, it would be very important to study the atomic bomb peak ^{14}C signal, which has a potential annual dating resolution[21] for the period since AD 1955". A study along these lines of a modern olive tree trunk and a living olive tree branch, albeit not from Santorini but from northern Israel, was recently conducted by Ehrlich et al.[22] They obtained near-annual resolution with radiocarbon measurements of modern olive wood using the radiocarbon 'bomb peak'. Their results show that ^{14}C dates along the olive wood circumference may differ by up to a few decades. Hence, ^{14}C dates of the outer tree-ring in olive wood do not necessarily represent the last year of growth! The authors, therefore, question the accuracy of radiocarbon dating olive wood in archaeological studies and in particular with regard to the ^{14}C date of the Minoan Santorini eruption based on an olive tree branch.[23]

All these new developments have repercussions for ^{14}C dating studies of the Hyksos period, the early 18th Dynasty and the Minoan Santorini eruption. Though we planned a full Bayesian sequence analysis of the new ^{14}C dates of Ashkelon in this article, right now we have to take a step back. There is no point using the current IntCal13 curve, which does not seem to facilitate accurate calibration for the period 1700–1500 BCE.[24] We have to wait for the new calibration curve IntCal19 to be completed, approved and released. Nevertheless, the uncalibrated ^{14}C dates we present constitute the basic measurement results in conventional radiocarbon years BP. These results remain valid, irrespective of calibration curves, and also facilitate excellent comparison between Ashkelon and Tell el-Dabʿa, though the time framework is relative in non-calendrical ^{14}C years BP.

Radiocarbon Dating Methodology at Groningen University

The radiocarbon measurements we present of Ashkelon are based on animal bones or (charred) plant seeds. For bone, the datable fraction is the organic matrix, collagen. The procedure for separating the collagen fraction is based on Longin.[25] The first step is an acid bath (4% HCl), followed by thorough washing with demineralized water. This is followed by a base wash (1% NaOH), followed by HCl (4%). Next, the collagen is dissolved in slightly acid demineralized water. The remaining solution is dried by evaporation in a stove, yielding the pure collagen.

8 Pearson et al. 2018.
9 Bietak and Höflmayer 2007; Warburton 2009; Wiener 2009; 2012; Bruins 2010; Höflmayer 2012; 2017; Kutschera et al. 2012; Manning 2014; Manning et al. 2014; Bietak 2015; 2016; Bruins and van der Plicht 2017.
10 Pearson et al. 2018, 5.
11 Manning et al. 2018.
12 Bronk Ramsey et al. 2010; Dee et al. 2010.
13 Manning et al. 2018.
14 Wacker et al. forthcoming.
15 Reimer et al. 2013.
16 Reimer et al. forthcoming.
17 Friedrich et al. 2006; Friedrich and Heinemeier 2009.
18 Cherubini et al. 2014.
19 Bruins and Van der Plicht 2014; Friedrich et al. 2014; Manning et al. 2014.
20 Bruins and van der Plicht 2014, 286.
21 Quarta et al. 2005.
22 Ehrlich et al. 2018.
23 Friedrich et al. 2006; Friedrich and Heinemeier 2009.
24 Pearson et al. 2018.
25 Longin 1971.

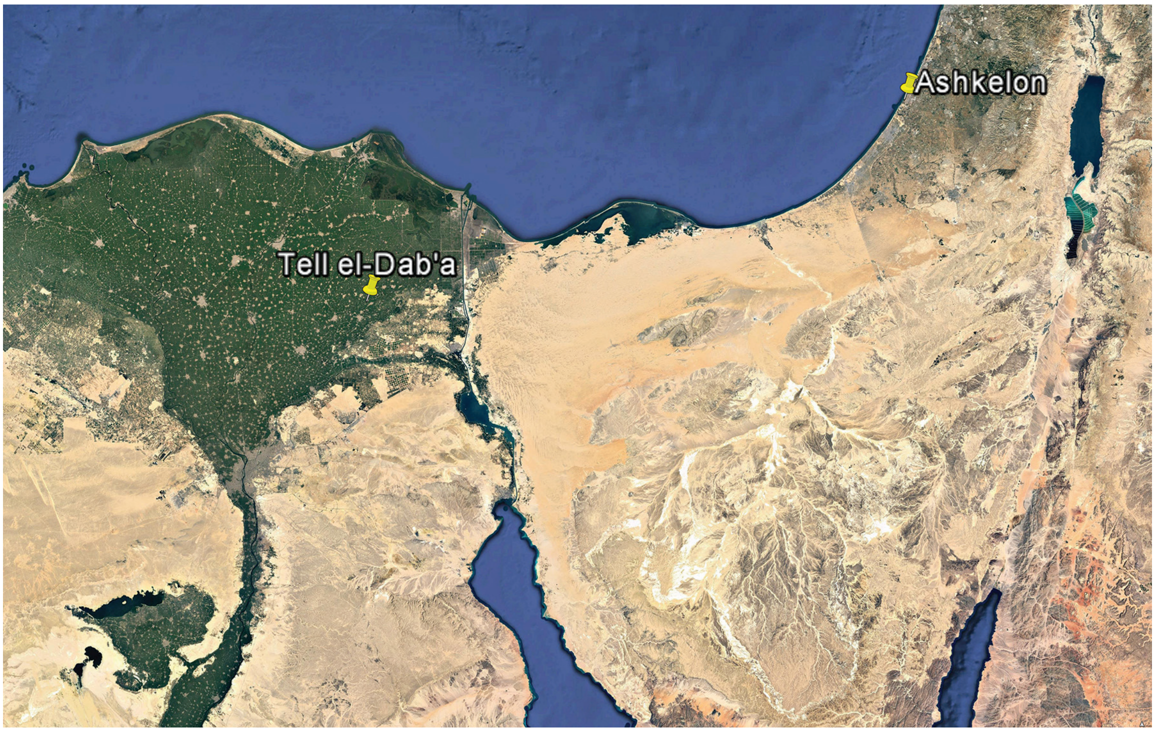

Fig. 1 Ashkelon was the major city-state along the south-eastern Mediterranean coast during the Middle Bronze Age [26], situated at a distance of c. 275 km from Tell el-Dabˁa, as the crow flies (© Google Earth)

The pretreatment procedure employed by Groningen for charred seeds is very similar to most other radiocarbon laboratories. The steps adhere to the ubiquitous acid-base-acid (ABA) framework. The first acid (HCl, 4% w/vol, 80°C) application is used to eliminate any geological carbonates that may have penetrated into the charred plant matrix. The sample is then rinsed to neutrality with ultra-pure water. The second step employs an alkaline solution (NaOH, 1% w/vol, RT), which dissolves any supramolecular polyphenols (mainly humic acids) that may have been absorbed from the soil. After a second rinse to neutrality, a final acid step is applied (HCl, 4% w/vol, 80°C) to ensure no atmospheric CO_2 absorbed during the alkaline phase remains in the reaction vessel. The sample is rinsed to neutrality once more and thoroughly dried.[27]

Approximately 4 mg of the pretreated material (collagen or seeds) are then weighed into tin capsules for combustion in an elemental analyser (EA, IsotopeCube NCS, Elementar®). The EA is coupled to an isotope ratio mass spectrometer (IRMS, Isoprime® 100), which allows the $\delta^{13}C$ value of the sample to be measured, and a fully automated cryogenic system that traps the CO_2 liberated on combustion. When the run is complete, the individual reaction vessels are transferred to a graphitization manifold, where a stoichiometric excess of H_2 gas (1: 2.5) is added, and the CO_2 gas is reduced to graphite over a Fe(s) catalyst.[28]

The graphite samples are then pressed into the cathodes employed by the accelerator mass spectrometer (AMS). The AMS in Groningen was replaced by a new machine in 2017. The old AMS is a 2.5 MV tandem accelerator, built by High Voltage Engineering Europa B.V.[29] The new AMS is a 0.2 MV compact system, a so-called MICADAS built by IonPlus.[30] Most Groningen dates in this contribution were measured by the old AMS. These dates can be recognized by their laboratory code GrA. A few dates were measured by the new AMS, using the laboratory code GrM. The new AMS is characterized by high efficiency resulting in excellent measurement precision (15–20 years BP). An illustrative example is an olive pit from Tomb Chamber 13 (Ashkelon Grid 50). It was split in two parts, whereby one part was measured with the new MICADAS system at Groningen University (GrM 12023, 3271 ± 15 BP) and the other half, for quality control and lab inter-comparison, at the tandem particle accelerator of Oxford University (OxA-36653, 3295 ± 30). The latter system is identical to the previous AMS at Groningen University. The above dating results of the olive pit by the two ^{14}C

26 Stager, Schloen and Master 2008.
27 Mook and Streurman 1983.
28 Aerts-Bijma et al. 2001.
29 Van der Plicht et al. 2000.
30 Synal et al. 2007.

Archaeo-historical age BCE	Egypt histori-cal association		Tell el-Dabʿa general phase	Ashkelon grid/local phase		Ashkelon stratigraphic period	Archaeological period
1460–1410	18th Dyn.		C/2	2/9	50/11	XIX	LB I
1500–1460	18th Dyn.		C/3				LB I
1530–1500	18th Dyn.		D/1	2/10		XX	MB IIC
1560–1530	15th Dyn. (Hyksos)		D/2	2/10	50/11	XX	MB IIC
1590–1560	15th Dyn. (Hyksos)		D/3				MB IIC
1620–1590	15th Dyn. (Hyksos)		E/1	2/11 Gate 4			MB IIB
1638–1620	15th Dyn. (Hyksos)		E/2				MB IIB
1680–1638	13th. Dyn.	King-dom of Avaris					MB IIB
			E/3	2/12 Gate 3		XXII	MB IIB
1710–1680	13th Dyn.	King-dom of Avaris	F				MB IIA–B
	13th Dyn.						

Tab. 1 Stratigraphic archaeological and historical correlations between Tell el-Dabʿa and Ashkelon, according to Bietak 2010; Bietak et al. 2008; Stager et al. 2008, 215–217; Stager 2018; Voss and Stager 2018. The focus is on the archaeological phases related to the Hyksos. However, also the neighbouring phases, preceding and postdating the 15th Dynasty, are included in our radiocarbon comparison. The thick solid line for Tell el-Dabʿa between Phases D/2 and D/1 signifies a stratigraphic archaeological hiatus in most excavated areas. At Ashkelon each Grid has its own Local Phase, which is linked across the entire site to defined Stratigraphic Periods, 24 in total (Stager et al. 2008, 215–217), representing its occupational history, labelled in Roman numerals from Period I (Mamluk and Ottoman) to Period XXIV (Canaanite, MB IIA, late 12th Dynasty). The dotted line for Ashkelon Grid 2 between Phases 10 and 9 signifies the lack of field stratigraphic data concerning the border between these phases. Ashkelon Grid 50, Local Phase 11 relates to tomb chambers cut in kurkar bedrock, containing multiple burials from different periods (MB IIB to LB I/II)

labs are indeed very similar. Archaeological details of this sample are presented below in the section about Ashkelon Grid 50, Tomb Chamber 13.

Archaeological Phases Associated with the 15th Dynasty (Hyksos) at Ashkelon and Tell el-Dabʿa

Based on studies of the respective material cultural remains, Bietak, Kopetzky, Stager and Voss[31] made a correlation between the Middle Bronze Age stratigraphy of Tell el-Dabʿa and Ashkelon (Tab. 1). We used the above synchronization, based on ceramics,[32] to compare the related phases between the two sites in terms of radiocarbon measurements, focusing on the 15th Dynasty.

The main Hyksos period (15th Dynasty) at the key site of Tell el-Dabʿa, identified as the Hyksos capital Avaris in the eastern Nile Delta, is associated by Bietak in archaeological terms with stratigraphic Phases E/2, E/1, D/3 and D/2 (Tab. 1). The beginning of the 15th Dynasty is placed by Bietak within Phase E/2.[33] Tell el-Dabʿa Phases E/2 and E/1 are related to MB IIB, in accordance with their respective material cultural content. The transition to MB IIC occurred in the middle of the subsequent Phase D/3.[34] The following Phase D/2 is understood by Bietak to continue until the end of MB IIC, associated with the conquest of Avaris by Ahmose and the beginning of the 18th Dynasty. Phase D/1 is considered to postdate the conquest of Avaris.[35] However, alternative associations between certain archaeological phases and Egyptian history have been discussed in detail by Aston.[36] For example, Phase D/1 may perhaps still belong to the Hyksos period and Phase C/3 could mark the beginning of

31 Bietak et al. 2008.
32 Bietak et al. 2008.
33 Bietak, Forstner-Müller and Mlinar 2003.
34 Bietak 1991, 57.
35 Bietak 2010.
36 Aston 2018.

Fig. 2 Ancient Ashkelon is surrounded by massive Middle Bronze Age earthen ramparts, reused in later periods.[37] The resulting semicircular outline of the city can be seen on this Google Earth Pro © image. Radiocarbon dates presented here are derived from organic samples excavated in Grid 2 at the North Tell and in Grid 50 at the South Tell. Houses of modern Ashkelon can be seen in the lower right-hand corner of the image

the 18th Dynasty.[38] Höflmayer[39] highlights that the palaces of Phases C/3 and C/2 were initially dated by Bietak[40] to the end of the Second Intermediate Period. Such dating is, in the view of Höflmayer, supported by radiocarbon evidence.[41] Here it should be added that all published radiocarbon calibrations and sequence analyses regarding Tell el-Dabʿa need to be redone after the new IntCal19 curve has been released.

At Ashkelon the main archaeological stratigraphic sequence for the Middle Bronze Age is situated at the North Tell, particularly in Grid 2[42] (Figs. 2, 3). Here Phase 12 (Gate 3), associated with the late 13th Dynasty, precedes Phase 11 (Gate 4) and Phase 10. The latter two phases are associated with the 15th Dynasty (Tabs. 1, 2, Fig. 2).

Unfortunately, the transition from the 15th to the 18th Dynasty does not show up clearly at Ashkelon in archaeological terms. The Stratigraphic Period XX at Ashkelon, associated with MB IIC, is represented at the North Tell (Grid 2) by Local Phase 10 (Tabs. 1, 2, Figs. 2, 3). The chronology attributed to MB IIC by the excavators of Ashkelon[43] is c. 1600–1550 BCE. The subsequent Local Phase 9 at the North Tell is understood to begin in Late Bronze (LB) I and continues for about 600 years(!) until Iron II. The related stratigraphic uncertainties are well expressed by Voss and Stager:[44] "The Phase 10 construction belongs to the last part of the Middle Bronze Age but its exact date and duration are difficult to determine on the basis of the material that is preserved. The centuries of erosion that followed, when the city's fortifications were neglected during the Late Bronze Age and the first part of the Iron Age I, resulted in the loss of the hypothesised Phase 10 glacis, which we were not able to detect".

The stratigraphic relations between Tell el-Dabʿa and Ashkelon, which seem well established for much of the Middle Bronze Age[45] appear, therefore, to be rather unclear at the transition from MB IIC to LB I and into the LB I period. This is indicated for Ashkelon in Table 1 by the dotted line between Local Phases 10 and 9 (Grid 2). We do not have radiocarbon dates, derived from the North Tell, related to the beginning of LB I, i.e., from the beginning of Phase 9.

37 Stager and Schloen 2008, 3–10.
38 Aston 2018, 34.
39 Höflmayer 2018, 162.
40 Bietak et al. 1994, 20–38.
41 Höflmayer 2018, 162–163.
42 Stager, Schloen and Master 2008; Stager et al. 2008, 217; Stager 2018; Voss and Stager 2018.
43 Stager et al. 2008, 217.
44 Voss and Stager 2018, 67.
45 Bietak et al. 2008.

Ashkelon stratigraphic period	North Tell Grid 2 (local phase)	South Tell Grid 50 (local phase)	Archaeological period	Association with dynastic Egypt	Archaeo-historical chronology BCE
XVIII	Phase 9	Phase 10	LB II	18th/19th Dyn.	c. 1400–1175
XIX	Phase 9	Phase 11	LB I	18th Dyn.	c. 1550–1400
XX	Phase 10	Phase 11	MB IIC	Late 15th Dyn.	c. 1600–1550
XXI	Phase 11	Phase 11	MB IIB	Early 15th Dyn.	c. 1650–1600
XXII	Phase 12	–	MB IIA	Late 13th Dyn.	c. 1725–1650

Tab. 2 Stratigraphic periods and local phases at Ashkelon, according to Stager et al. 2008, 215–217. Ashkelon Stratigraphic Periods XXI and XX are related to the 15th Dynasty.

This lack at the North Tell of archaeological strata and radiocarbon data for the transition from MB IIC to LB I is compensated for to some extent by a necropolis situated at the South Tell of Ashkelon in Grid 50 (Fig. 2). Here various rock-cut tomb chambers with multiple burials have been excavated, showing well-preserved ceramic remains ranging from MB IIB to LB I/LB II.[46] The food remains that accompanied these burials from the Hyksos period and the 18th Dynasty provided excellent short-lived material (olive pits) for radiocarbon dating. We present in this contribution ^{14}C results of Tomb Chamber 13. The individual radiocarbon dates show the ^{14}C time range during which this tomb was used in MB II and LB I, which constitutes important autonomous chronological information. The ^{14}C results of each Grid are presented separately in the next sub-chapters (Tabs. 3, 4). Thereafter, all Ashkelon dates, both from Grid 2 and Grid 50, are arranged in chrono-stratigraphic sequence in comparison with the Tell el-Dabʿa dates in uncalibrated ^{14}C years BP (see Tab. 5).

Ashkelon North Tell, Grid 2: Uncalibrated Radiocarbon Dates

The uncalibrated ^{14}C dates of Ashkelon Grid 2 are consistent with the archaeological stratigraphy (Tab. 3). The earliest radiocarbon dates were indeed obtained for Phase 12 (Gate 3), which is the earliest stratigraphic phase of Ashkelon included in the present study.

The next stage, Ashkelon Phase 11 (Gate 4), is represented by seven uncalibrated radiocarbon dates. Six dates form an internally consistent group (Tab. 3), ranging from 3445 ± 35 BP (GrA-46423) to 3390 ± 35 BP (GrA 34267). The latest date (3330 ± 35 BP, GrA 46409) is from a fill in Gate 4 (Footgate) and may belong to Phase 11, as suggested by the excavators, or perhaps to Phase 10, as suggested by the ^{14}C date.

Ashkelon Grid 2, Phase 10 is so far problematic in terms of radiocarbon dating. A mixed bin fill, containing Middle Bronze and Iron I pottery, assigned by the excavators in part to Phase 10, also yielded animal bones. The archaeological context is far from ideal, but here suitable short-lived organic material was available for radiocarbon dating. One animal bone (GrA 34459, 3310 ± 60 BP) yielded the latest ^{14}C Bronze Age result in our series of Grid 2, which seems to fit with Phase 10. However, the other bone sample of a sheep or goat (GrA 46407, 3440 ± 35 BP) is significantly earlier and appears more likely to belong to Phase 11.

Ashkelon South Tell, Grid 50: Radiocarbon Dating of Tomb Chamber 13

Unfortunately, Grid 2 Phase 10, associated with the MB IIC archaeological period, lacks samples so far for our radiocarbon research. However, we have dates also from the Middle–Late Bronze necropolis in Grid 50,[47] situated in the southern part of Tel Ashkelon (Fig. 2). This necropolis is characterized by a complex of tomb chambers cut in local calcified sandstone (kurkar) bedrock. Phase 11 in Grid 50 is the designation given by the excavators to subterranean tombs with material cultural remains from MB IIB, MB IIC, LB I and the LB I/LB II transition. It seems that the necropolis was used continuously from c. 1700 to 1400 BCE. However, multiple changes were noted in burial practices.[48]

We present here 10 radiocarbon measurements of Tomb Chamber 13 (Tab. 4). This chamber is part of a complex that includes also Chambers 14 and 16.[49] The tombs were used for multiple burials during the above periods. Earlier burials were often pushed aside to make room for new interments. Hence, a stratigraphic differentiation is usually not feasible. Each burial was apparently accompanied by a funerary meal and food offerings, as attested by grape seeds, olive pits and animal bones associated with individual interments. We dated olive pits from different spatial positions (Tab. 4) within Tomb Chamber 13 in order to obtain a chronological picture of the time range of different burials. The age of an olive pit should be similar as the time of the related interment.

46 Stager et al. 2008, 299–303.

47 Stager et al. 2008, 299–303.

48 Ibidem.

49 Ibidem, 300.

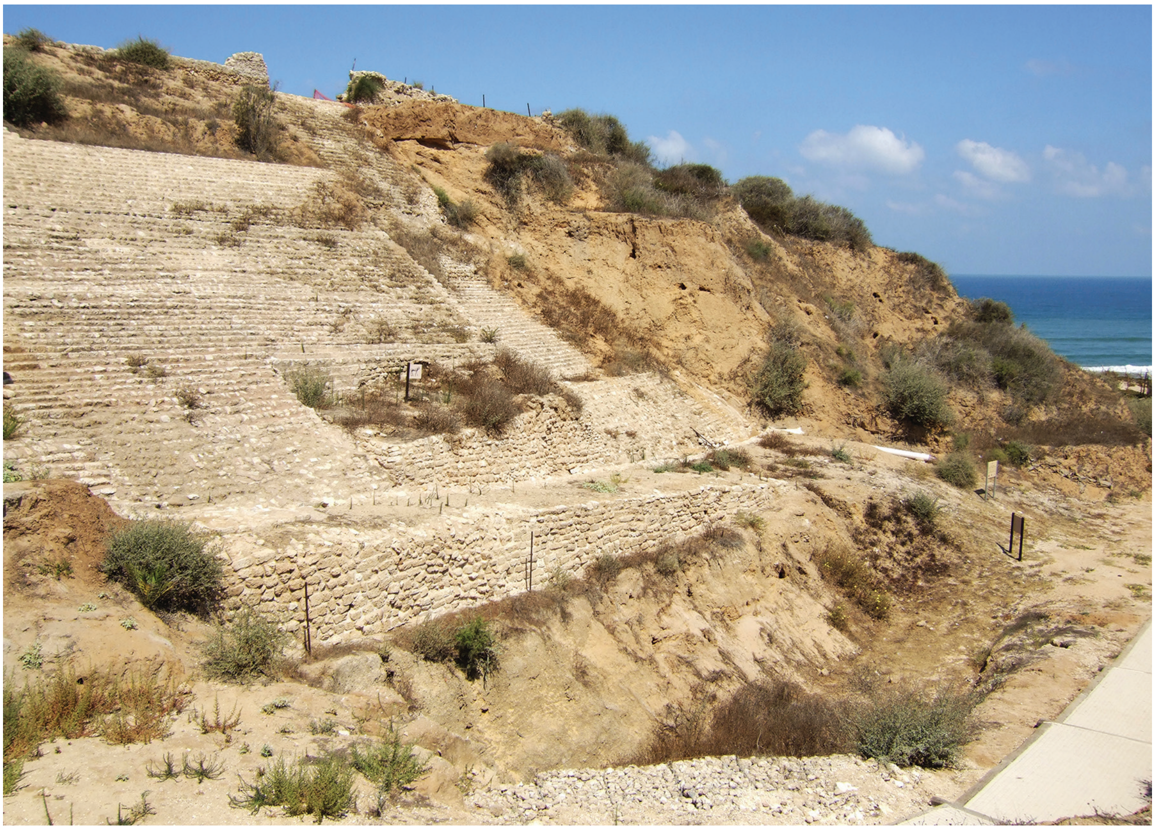

Fig. 3 The northern slope of the North Tell at Ashkelon, showing the outline of the prominent Middle Bronze Age defence wall (glacis). A dry moat existed at the bottom of the glacis. The visible stone cover is from a much later reuse of the glacis in medieval times (Fatimid and Crusader periods). The stratified Middle Bronze Age samples for radiocarbon dating from Phases 12, 11 and 10, presented in this paper, are derived from Grid 2, which covers the glacis slope and the area above it on top of the North Tell. The Mediterranean Sea is visible nearby to the west (photo by H.J. Bruins, 14 July 2009)

Our radiocarbon dates are derived from three different spatial positions in Tomb Chamber 13: (a) centre – south, (b) near Body 167 and (c) east. The earliest ^{14}C dates are from the eastern area of the tomb chamber. Comparing the conventional ^{14}C results with those from Grid 2 (Tab. 3), it is clear that the earliest four dates of Tomb Chamber 13 (3440 ± 45 BP to 3380 ± 35 BP) are similar to those for Phase 11 (3445 ± 35 BP to 3390 ± 35 BP), associated with MB IIB and the early/middle 15th Dynasty.

The next ^{14}C time cluster in Tomb Chamber 13, also from its eastern area, comprises two dates: 3325 ± 35 BP (GrA 40915) and 3335 ± 35 BP (GrA 40916). Compared with Ashkelon Grid 2 (Tab. 3), these ^{14}C dates may relate to the transition from Phase 11 to Phase 10 (MB IIB to MB IIC).

Another spatial position in Tomb Chamber 13, near Body 167, yielded a somewhat later time period. Two dates, 3271 ± 15 BP (GrM 12023) and 3300 ± 15 BP (GrM 12024), were measured with the new MICADAS-17 accelerator mass spectrometer at Groningen University. Both dates have a very small standard deviation (15 yr BP), which is typical of the performance of the new system. One olive pit was split in two parts and measured for quality control both in Groningen (GrM 12023) and Oxford (OxA-36653). The results are similar: 3271 ± 15 BP and 3295 ± 30 BP, respectively. Indeed, all three dates for olive pits near Body 167 are identical. Compared with the ^{14}C results of Tell el-Dabʿa and Ashkelon Grid 2 (Tab. 5), Body 167 was most likely buried during the late 15th Dynasty (MB IIC).

The latest date for Tomb Chamber 13 is 3248 ± 15 BP (GrM 12025). The olive pit that yielded this date is derived from a centre south spatial position. The uncalibrated ^{14}C date is *younger* than any of the other ^{14}C dates of Ashkelon and Tell el-Dabʿa (Tab. 5) and may chronologically relate to either MB IIC or LB I.

Radiocarbon Dating Comparée of Hyksos-Related Phases at Ashkelon and Tell el-Dabʿa

Concerning Tell el-Dabʿa, the first radiocarbon dates were measured in the late 1980s on charcoal samples by Dr. Edwin Pak at the Institut für Radiumforschung und Kernphysik (University of Vienna). The charcoal is

Archaeo-period & dynasty	Ashkelon stratigraphic period	Grid & phase	Archaeological context	Material	Groningen Lab no.	δ^{13}C (‰)	^{14}C age (yr BP)
MB IIC Late 15th	XX	2/10	Bin fill, mixed MB & Iron I pottery, Sq 44, L139, B175	Animal bone	GrA 34459	-18.34	3310 ± 60
MB IIC Late 15th	XX	2/10	Bin fill, mixed MB & Iron I pottery, Sq 44, F139. L139, B175	Sheep/ goat bone	GrA 46407	-19.41	3440 ± 35
MB IIB Early 15th	XXI Gate 4	2/11	Fill in Footgate, Sq 85, L99, B36, 48, 53	Cattle bone	GrA 46409	-19.36	3330 ± 35
MB IIB Early 15th	XXI Gate 4	2/11	Destruction debris or occupational de-bris, Sq 55, FG68, L146, B228	Sheep bone, cal-caneus	GrA 34267	-19.48	3390 ± 35
MB IIB Early 15th	XXI Gate 4	2/11	Destruction debris or occupational debris, Sq 55, FG4, L146, B259	Cattle bone, pelvis	GrA 34461	-20.23	3410 ± 490
MB IIB Early 15th	XXI Gate 4	2/11	Burial, Sq 66, L178, B8, #48, 679	Grape pips	GrA 40728	-26.31	3400 ± 30
MB IIB Early 15th	XXI Gate 4	2/11	Burial, Sq 66, L178, B8, #48, 679	Grape pips	GrA 40731	-23.73	3430 ± 30
MB IIB Early 15th	XXI Gate 4	2/11	Burial, Sq 66, L178, B8, #48, 679	Grape pips	GrA 40730	-24.65	3440 ± 30
MB IIB Early 15th	XXI Gate 4	2/11	Floor with occupa-tional debris, Sq 85, L/F90, B50, 52, 57	Bone	GrA 46423	-23.12	3445 ± 35
MB IIA Late 13th	XXII Gate 3	2/12	Fill, Sq 56, L10, B33	Cattle bone	GrA 46488	-19.66	3455 ± 35
MB IIA Late 13th	XXII Gate 3	2/12	Foundation fill for Gate 3, Sq 85, L43, B60	Animal bone	GrA 34248	-18.78	3525 ± 40
MB IIA Late 13th	XXII Gate 3	2/12	Fill in Gate, Sq 85, L38, B31, 84	Sheep/ goat bone	GrA 46410	-17.83	3530 ± 35

Tab. 3 Radiocarbon dated samples of Ashkelon Grid 2, situated at the North Tell. The archaeological context of the samples, the type of organic material and the conventional radiocarbon measurements (uncalibrated) are presented with their δ^{13}C values. The term bin fill, used by the excavators, signifies a kind of waste container (bin), containing fill material.

Archaeo-period & dynasty	Ashkelon stratigraphic period	Grid & phase	Archaeological context inside Tomb Chamber 13	Material	Groningen & Oxford Lab no.	$\delta^{13}C$ (‰)	^{14}C age (yr BP)
MB–LB 15th–18th	XXI–XIX	50/11	Centre south, Sq 58L, L517, F423, B44, #54203	Olive pit	GrM 12025	-20.26	3248 ± 15
MB–LB 15th–18th	XXI–XIX	50/11	Near body 167, Sq 58L, L517, F423, B28, #53958a	Olive pit, split half #1	GrM 12023	-22.36	3271 ± 15
MB–LB 15th–18th	XXI–XIX	50/11	Near body 167, Sq 58L, L517, F423, B28, #53958a	Olive pit, split half #2	OxA-36653	-23.03	3295 ± 30
MB–LB 15th–18th	XXI–XIX	50/11	Near body 167, Sq 58L, L517, F423, B28, #53958b	Olive pit	GrM 12024	-21.16	3300 ± 15
MB–LB 15th–18th	XXI–XIX	50/11	East, Sq 58L, F423, L517, B87, #55,122	Olive pits	GrA 40915	-22.76	3325 ± 35
MB–LB 15th–18th	XXI–XIX	50/11	East, Sq 58L, F423, L517, B87, #55,122	Olive pits	GrA 40916	-20.72	3335 ± 35
MB–LB 15th–18th	XXI–XIX	50/11	East, Sq 58L, F423, L517, B114, #56,619	Olive pits	GrA 40922	-27.17	3380 ± 35
MB–LB 15th–18th	XXI–XIX	50/11	East, Sq 58L, F423, L517, B87, #55,122	Olive pits	GrA 40917	-21.47	3390 ± 35
MB–LB 15th–18th	XXI–XIX	50/11	East, Sq 58L, F423, L517, B114, #56,619	Olive pits	GrA 40919	-23.68	3405 ± 35
MB–LB 15th–18th	XXI–XIX	50/11	East, Sq 58L, F423, L517, B114, #56,619	Olive pits	GrA 40921	-24.11	3440 ± 45

Tab. 4 Ashkelon Grid 50, Phase 11. Conventional radiocarbon dating results of different areas of Tomb Chamber 13, used from MB II until LBI/II. The dates are ordered chronologically from late to early

mainly from acacia trees, used as firewood in different strata at the site.[50] There are 15 samples derived from Area F/1, the new centre at Tell el-Dabʿa with a Middle Bronze Age population. These samples range from Local Phase e (General Phase N), associated with the 12th Dynasty, until Local Phase b/1–2 (General Phase E/3–E/2), associated with the end of the 13th Dynasty and the first part of the 15th Dynasty (b/1 is Hyksosian). One sample is from Area A (Eastern Town), Local and General Phase F (~ b/3 in F/1), associated with the Kingdom of Nehesy (late 13th Dynasty). The ^{14}C measurements were evaluated by Bruins[51] in relation to the archaeological stratigraphy of Tell el-Dabʿa.[52] The dates are far from ideal, having a large standard deviation of more than 100 radiocarbon years, besides being based on charcoal. Nevertheless, sequence modelling managed to make some sense out of the wide-ranging results. The sequence model indicated that most results are earlier than archaeo-historical dating by roughly 100 to 200 years. However, the large standard deviation of the individual ^{14}C dates and the possible old-wood effect of charcoal precluded definitive conclusions.[53]

Subsequent radiocarbon research by Kutschera et al.[54] of Tell el-Dabʿa, based on some 40 short-lived seed samples of annual grasses (*Poaceae*) gave significant scientific results. The standard deviation of individual samples, measured at the Vienna Environmental

50 Bietak, personal communication, 28 March 1988.
51 Bruins 2007.
52 Bietak 1991; 1997.
53 Bruins 2007.
54 Kutschera et al. 2012.

Association with dynastic Egypt	Tell el-Dabʿa general phase	^{14}C lab no.	^{14}C age (yr BP)	Ashkelon grid/local phase	^{14}C lab no.	^{14}C age (yr BP)
				50/11	GrM 12025	3248 ± 15
18th Dyn.	**C/2**	VERA 3031	3414 ± 35	**50/11**	*GrM 12023	3271 ± 15
				50/11	*OxA-36653	3295 ± 30
				50/11	*w. mean	3276 ± 13
18th Dyn.	**C/3**	(C/2–3)				
		*VERA 3724	3320 ± 29			
		*OxA-15959	3296 ± 31	**50/11**	GrM 12024	3300 ± 15
		*OxA-15957	3322 ± 31			
		*w. mean	3313 ± 17	**2/10**	GrA 34459	3310 ± 60
18th Dyn.	**D/1**	VERA 3032	3314 ± 36	**50/11**	GrA 40915	3325 ± 35
15th Dyn.	**D2**	VERA 3616	3337 ± 44	**2/11**	GrA 46409	3330 ± 35
		VERA 2628	3359 ± 34	**50/11**	GrA 40916	3335 ± 35
		VERA 2627	3390 ± 34			
		VERA 3622	3394 ± 36	**50/11**	GrA 40922	3380 ± 35
		*VERA 3621	3354 ± 26	**50/11**	GrA 40917	3390 ± 35
		*OxA-15953	3392 ± 31			
		*OxA-15901	3479 ± 33			
		*w. mean	3399 ± 37			
	D/3–D/2	VERA 3645	3351 ± 38			
15th Dyn.	**D/3**	VERA 3620	3377 ± 33			
		VERA 2629	3384 ± 30			
		VERA 3619	3396 ± 34			
		VERA 2895	3426 ± 26			
		VERA 2896	3428 ± 37			
		VERA 3033	3480 ± 28	**2/11**	GrA 34267	3390 ± 35
15th Dyn.	**E/1**	VERA 2626	3389 ± 36	**2/11**	GrA 40728	3400 ± 30
		VERA 3617	3422 ± 35	**50/11**	GrA 40919	3405 ± 35
		VERA 3636	3449 ± 26	**2/11**	GrA 40731	3430 ± 30
		*VERA 3618	3436 ± 35	**2/10**	GrA 46407	3440 ± 35
		*OxA-15949	3437 ± 30	**2/11**	GrA 40730	3440 ± 30
		*OxA-15948	3511 ± 32	**50/11**	GrA 40921	3440 ± 45
		*w. mean	3462 ± 25	**2/11**	GrA 46423	3445 ± 35
15th Dyn.	**E/2**	VERA 3637	3415 ± 26			
13th Dyn.	**E/3**	VERA 2897	3525 ± 26	**2/12**	GrA 46488	3455 ± 35
	F–E/3	VERA 3643	3450 ± 26	**2/12**	GrA 34248	3525 ± 40
13th Dyn.	**F**	VERA 2625	3467 ± 35	**2/12**	GrA 46410	3530 ± 35
		VERA 2898	3505 ± 27			

Tab. 5 The uncalibrated ^{14}C dates of Tell el-Dabʿa are arranged as published by Kutschera et al. 2012. Archaeological phases and their association with Egyptian dynastic history are indicated (based on Bietaket al. 2008, Bietak 2010, and Stager, Schloen and Master 2008). The thick solid line for Tell el-Dab'a between Phases D/2 and D/1 signifies a stratigraphic archaeological hiatus. The uncalibrated 14C dates of Ashkelon are arranged chronologically from late to early, more or less placed in a position vis-a-vis similar dates of Tell el-Dab'a. The transition from 15th to 18th Dynasty is unclear with regard to Ashkelon, as explained in the text. Therefore, no horizontal line is placed in the table for Ashkelon concerning the position of this transition. An asterisk (*) signifies duplicate measurements of the same sample and the resulting weighted mean.

Research Accelerator (VERA) Laboratory (University of Vienna) with 10 duplicate measurements taken at the Oxford Radiocarbon Accelerator Unit (University of Oxford), ranged from 25 to 44 radiocarbon years BP. These are high-quality dates that covered the stratigraphy of Tell el-Dabʿa from General Phase N/2–3 to C/2. Sequence modelling showed the radiocarbon dates to be earlier along all the phases by c. 120 calendar years.[55] However, calibration and modelling has to be redone when the new IntCal19 curve will have become available, as described above.

The conventional uncalibrated ^{14}C dating results for Ashkelon and Tell el-Dabʿa are presented in Table 5, facilitating comparison between the two archaeological sites. Concerning Ashkelon Grid 2, we have so far only two radiocarbon dates for Phase 10 that differ widely from each other. There are no ^{14}C dates for Phase 9, which anyhow is designated to cover a very long time period of c. 600 years(!) from 1550 to 950 BCE, including LB I, LB II and Iron I. Therefore, Phase 10 of Ashkelon Grid 2 is, unfortunately, not well represented by radiocarbon dates.

Ashkelon Phase 12 and Tell el-Dabʿa Phases F and E/3 (13th Dynasty, MB IIA/B)

The uncalibrated radiocarbon dates of Ashkelon Phase 12 and Tell el-Dabʿa Phases F and E/3 are indeed very similar (Tab. 5). Hence, the stratigraphic correlation between these phases, based on ceramic similarities,[56] is hereby supported independently by radiocarbon dating.

Ashkelon Phase 12 is characterized by the largest gate (Gate 3) of the Middle Bronze Age sequence at the North Tell in Grid 2. The complete gate structure, built entirely of mud-bricks, was c. 35.5 m long and 12 m wide.[57] Pottery of Phase 12 includes Marl C jars with corrugated rims of 13th Dynasty type. A stratigraphic correlation with Tell el-Dabʿa Phase F is provided by a Marl C *zir* of type 4. The founding of Gate 3 is dated in terms of archaeological classification to the end of MB IIA, but the excavators also suggested alternative classification options: transitional MB IIA/B or early MB IIB.[58]

Tell el-Dabʿa Phase F shows many important novel developments.[59] The 'villa' house type is introduced and social differentiation becomes apparent. Courtyards are used for grain silos, stores and other domestic purposes, as well as for burials.[60] About 40 percent of the ceramic assemblage is of MB IIA types, but some MB IIB styles also occur.[61] A completely new building period occurred in Area A/II, which was deserted at the end of the previous Phase G. Here, one of the largest Middle Bronze Age temples in the eastern Mediterranean region was built (Temple III). This temple has been attributed by Bietak to King Nehesy, as two limestone door-jambs bearing his name were found within the area of the sacred precinct around the temple.[62]

Nehesy appears on the Turin King List, on the first line of column 9 after a lacuna. The preceding column 8 contains only kings of the 13th Dynasty, although the last two lines are severely damaged and we do not know their content. Therefore, it is uncertain whether Nehesy and the subsequent kings belong to the 13th or 14th Dynasty.[63] The entirety of column 9 and the first 20 lines of column 10 are dedicated to the successors of King Nehesy. It is understood that line 21 contains the summation of the 14th Dynasty, but only a small fragment is preserved.[64]

The writings of Manetho mention the 14th Dynasty as "76 kings of Xois".[65] Given the above lacunas in the Turin King List, various interpretations exist among Egyptologists regarding the 14th Dynasty. Ryholt considers it the first dynasty of Asiatic origin in the north-eastern Nile Delta,[66] more or less parallel in time with the length of the 13th Dynasty, which ruled over the rest of Egypt. However, Allen strongly disagrees and places the beginning of the 14th Dynasty after the end of the 13th Dynasty or, perhaps, overlapping only during the last kings of the latter dynasty.[67]

The subsequent Phase E/3 at Tell el-Dabʿa shows an enlargement of the villas in Area F/I. In addition to the large Temple III, a second temple (V) with an altar was built in the best Canaanite tradition. Nearly all MB IIA types have disappeared in the ceramic assemblage, as MB IIB is clearly dominant.[68]

Ashkelon Phase 11 and Tell el-Dabʿa Phases E/2, E/1 and D/3 (15th Dynasty, MB IIB)

These archaeological strata are associated with the early and middle parts of the 15th Dynasty. Ashkelon Phase 11 (Gate 4) had a much smaller mud-brick gate, carved out of the massive towers and side walls of the upper gate in Phase 12 (Gate 3). The entrance between the piers was only 1.5 m wide. Gate 4 was, therefore, accessible mainly for pedestrians.[69] The ceramic assemblage of Phase 11 includes, according to

55 Kutschera et al. 2012.
56 Bietak et al. 2008.
57 Voss and Stager 2018, 24–103.
58 Stager et al. 2008, 232.
59 Bietak 1991, 40.
60 Bietak 1991, 38–40; 1997, 105–109. Cf., as well, Prell in this volume.
61 Bietak 1991, 39–40.
62 Bietak 1991, 39; 1997, 109.
63 Ryholt 1997, 94–97.
64 Ryholt 1997, 95.
65 Allen 2010, 2.
66 Ryholt 1997, 94.
67 Allen 2010, 5.
68 Bietak 1991, 40.
69 Stager et al. 2008, 234.

Voss and Stager (2018), "a Cypriot Red-on-Black bowl fragment, Cypriot White Painted III–IV jug fragments, a Cypriot White Painted IV–V jug fragment, Egyptian Marl C zirs of rim Type 5, Nile E2-fabric cooking pots, and an Egyptian Biconical-3 Tell el-Yahudiyah juglet fragment. All of these forms have parallels in Tell el-Dabʿa Phases E/2–D/3".[70]

We have six radiocarbon dates for Ashkelon Phase 11 and there are 13 radiocarbon measurements for the correlating Tell el-Dabʿa Phases E/2, E/1 and D/3[71]. Comparing the uncalibrated ^{14}C dates of both sites (Tab. 4), we may conclude again that the dating results are quite similar, with the exception of one Ashkelon date (GrA 46409), which is considerably later than all the other 18 dates. This date, 3330 ± 35 BP, is from a cattle bone excavated in the fill of Gate 4. Perhaps the fill belongs to the subsequent Phase 10, to which the date would fit better in chronological ^{14}C terms. Nevertheless, the great majority of the ^{14}C results confirm that Ashkelon Phase 11 and Tell el-Dabʿa Phases E/2, E/1 and D/3 can be considered synchronous also in terms of radiocarbon dating, which is an independent confirmation of the ceramic correlations.

Concerning Tomb Chamber 10 (Ashkelon Grid 50), two radiocarbon dates (3405 ± 35 BP, GrA 40919 and 3440 ± 45 BP, GrA 40921) fit well (Tab. 4) with the other dates of Ashkelon Grid 2, Phase 11 and Tell el-Dabʿa Phases E/2, E/1 and D/3, associated with MB IIB and the early to middle 15th Dynasty.

Ashkelon Phase 10 and Tell el-Dabʿa Phase D/2 (15th Dynasty, MB IIC)

These interrelated phases are considered to coincide with the late part of the 15th Dynasty (coinciding more or less with the archaeological period MB IIC). A stratigraphic archaeological hiatus is associated by Bietak with the end of Hyksos rule at Avaris (Tell el-Dabʿa),[72] though alternative interpretations have recently been suggested also by Aston[73] and Höflmayer.[74] The archaeological period MB IIC at Tell el-Dabʿa includes, according to Bietak,[75] the late part of Phase D/3 and Phase D/2 and also Phase D/1, though the latter is related to the 18th Dynasty and not to the 15th Dynasty (Tab. 1).

Concerning Ashkelon Grid 2, the end of Phase 10 is more elusive in stratigraphic terms and precise archaeological dating is difficult,[76] as described above. The ceramics of Ashkelon Phase 10 is typical of MB IIC,[77] like Phase D/2 at Tell el-Dabʿa.[78] The ceramic assemblage at Ashkelon includes Tell el-Yahudiyeh ware, such as Biconial 2 and 3 juglets, similar to those found at Tell el-Dabʿa between Phases E/2 and D/3–D/2. Imports from Cyprus include White Painted III–IV in both Cross Line and Pendent Line Styles. Typical of the Middle Cypriot III–Late Cypriot I transition is White Painted V ware. Wheel-made cooking pots with fine sand filler fabric and outwards-rolled rims continue in Phase 10, as well as Egyptian Marl C3 clay zirs of Type 5.[79]

We have so far only two radiocarbon dates for Ashkelon Grid 2, Phase 10. Moreover, these two dates of animal bones from a bin fill differ widely. The earliest date, 3440 ± 35 BP (GrA 46407), would seem to fit better in terms of radiocarbon chrono-stratigraphy with the previous Phase 11 (Tab. 5). The other date, 3310 ± 60 BP (GrA 34459), is later than the Tell el-Dabʿa radiocarbon dates for Phase D/2 (Tab. 5). This seems significant, as Ashkelon Phase 10 covers a larger time frame than Tell el-Dabʿa Phase D/2 and is also correlated with the later Phase D/1 in the ceramic synchronization of phases at both sites.[80] Therefore, radiocarbon dating (Tab. 5) also supports the stratigraphic correlation between Ashkelon Phase 10 (3310 ± 60 BP, GrA 34459) and Tell el-Dabʿa Phase D/1 (3314 ± 36 BP, VERA 3032).

There are eight ^{14}C measurements for Tell el-Dabʿa Phase D/2.[81] It is clear that seven dates form a homogenous set, but OxA-15901 seems an outlier, being considerably earlier. Although we lack robust ^{14}C dates of Ashkelon Grid 2, Phase 10, several radiocarbon dates of Tomb Chamber 10 (3380 ± 35, GrA 40922; 3390 ± 35, GrA 40917) fit very well with ^{14}C dates of Tell el-Dabʿa Phase D/2 (Tab. 5).

The youngest radiocarbon dates at Ashkelon are from Tomb Chamber 13. One date (3248 ± 15 BP, GrM 12025) is significantly later than the youngest ^{14}C date of Tell el-Dabʿa (Tab. 5). The dates near Body 167 (Tab. 4) are slightly later than the Tell el-Dabʿa ^{14}C dates of Phases C/2–3 (Tab. 5).

The only ^{14}C date of Tell el-Dabʿa Phase C/2 proper (3414 ± 35 BP, VERA 3031) is clearly an outlier and would fit much better in chronological ^{14}C terms with Phase D/3. Unfortunately, the precise archaeological context of each radiocarbon date of Tell el-Dabʿa has not been published so far. Only the association is given with the general phase, but not the excavation area and local stratigraphic details. Therefore, we cannot assess the possible reason why VERA 3031 (Phase C/2) is much earlier, by c. 100 years BP, than the other ^{14}C dates for Phases C/2–3 and D/1 (Tab. 5).

70 Voss and Stager 2018, 63.
71 Kutschera et al. 2012.
72 Bietak 2010.
73 Aston 2018.
74 Höflmayer 2018.
75 Bietak 2010.
76 Voss and Stager 2018, 67.
77 Stager et al. 2008, 236.
78 Bietak et al. 2008.
79 Stager et al. 2008, 236.
80 Bietak et al. 2008, 57–59 and fig. 9.
81 Based on the uncalibrated ^{14}C dates of Tell el-Dabʿa published by Kutschera et al. (2012).

Discussion and Conclusions

A comparative analysis of interrelated Hyksos phases at Ashkelon and Tell el-Dabʿa, based on uncalibrated radiocarbon dates yielded significant results. These basic radiocarbon measurements remain valid, irrespective of the calibration curve, and can be compared with each other in terms of methodology. However, the timescale is relative, representing conventional ^{14}C years BP but not calendar years.

The earliest phases evaluated in this article, preceding the 15th Dynasty, are Ashkelon Grid 2, Phase 12 (Gate 3) and the related Tell el-Dabʿa Phases F and E/3. The material culture for these phases covers late MB IIA to early MB IIB.[82] The respective uncalibrated radiocarbon dates are very similar for both sites. Therefore, it can be concluded that ^{14}C dating fully supports their stratigraphic correlation, based on ceramics, albeit in relative chronological terms.

The 15th Dynasty is understood to begin during Phase E/2 at Tell el-Dabʿa and continue during Phases E/1 and D/3. These strata have been correlated with Ashkelon Grid 2, Phase 11 (Gate 4), according to their material cultural similarities, typical of MB IIB.[83] Also for these phases, radiocarbon dating gives analogous uncalibrated dates at both sites, fully backing the archaeological correlations in relative chronological terms.

The later part of the 15th Dynasty is generally associated with the archaeological period MB IIC. Ashkelon Grid 2, Phase 10 and Tell el-Dabʿa Phases D/2 and D/1 have been correlated on the basis of ceramic similarities.[84] But here the historical and archaeological relationships become more complex, as the end of the 15th Dynasty is understood by Bietak[85] to occur at the end of Phase D/2, whilst at Ashkelon the end of MB IIC is placed at the end of Grid 2, Phase 10, which, however, cannot be pinpointed at Ashkelon in terms of archaeological stratigraphy.[86] Therefore, the transition from the 15th Dynasty to the 18th Dynasty has not been clearly established at Ashkelon Grid 2. Concerning Tell el-Dabʿa, the position of this important historical boundary has been suggested at different archaeological and stratigraphic positions by different authors.[87] Our current radiocarbon dating study of Ashkelon has not been able to obtain clear results for Grid 2, Phase 10, due to lack of organic samples. The two dating results obtained differ considerably from each other and are not from an ideal stratigraphic context.

On the other hand, for Ashkelon Grid 50, Phase 11, we have a robust series of ten ^{14}C dates of Tomb Chamber 10. Comparing these uncalibrated dates with those of Tell el-Dabʿa and Ashkelon Grid 2, it becomes clear that Tomb Chamber 10 was used during the 15th Dynasty and also during the early 18th Dynasty.

Our current study is unable to provide new insights concerning the chronological position of the boundary between MB IIC and LB I at Ashkelon. More radiocarbon dates of Ashkelon Grid 2, Phase 10 may provide a better radiometric chronological picture. In addition, it would be useful to have more detailed contextual archaeological information of the organic samples from Tell el-Dabʿa used for radiocarbon dating, as only the general phases are given,[88] but not the respective areas of excavation with the local stratigraphy and sample context.

When the new calibration curve IntCal19 has been completed, approved and released, at some time during 2019, a follow-up study is possible. Then, the above uncalibrated radiocarbon dates can be calibrated into calendar years, using improved dendrochronological datasets based on many new measurements, also involving single year tree-ring ^{14}C data from different geographical regions. Bayesian sequence analyses may further enhance calibrated chronological precision in calendar years.

Acknowledgements

The radiocarbon dating of samples from Ashkelon was partly funded by the Gerda Henkel Foundation in the context of a project (AZ 52/F/15) by the first author. We thank the laboratory staff of the Centre for Isotope Research at Groningen University for their professional treatment and measurement of the samples. We are grateful to Michael W. Dee (Groningen University) for his supervision concerning a number of samples that were measured with the new MICADAS radiocarbon dating AMS system. We thank Christopher Bronk Ramsey and his staff at Oxford University for measuring a duplicate sample for quality control and lab intercomparison. We acknowledge the unique contribution of the chief excavators at Ashkelon – Lawrence Stager – and at Tell el Dabʿa – Manfred Bietak – as well as the many archaeologists and volunteers, who painstakingly excavated at these important sites during many seasons, gradually exposing a wealth of archaeological strata and objects, including organic materials that facilitated radiocarbon dating. We are grateful to Daniel M. Master (co-director of the Ashkelon excavations 2007–2016) and to Ross J. Voss (grid supervisor at the Ashkelon excavations 1986–2000; Ashkelon archaeological lab director 2000–2007) for providing contextual archaeological details of organic samples used for radiocarbon dating. We thank the reviewers and editors for their comments and the resulting improvement of the text.

82 Bietak et al. 2008.
83 Bietak et al. 2008.
84 Bietak et al. 2008.
85 Bietak 2010.
86 Stager et al. 2008, 217; Voss and Stager 2018.
87 Bietak 2010; Aston 2018; Höflmayer 2018.
88 Kutschera et al. 2012.

Bibliography

Aerts-Bijma, A.T., van der Plicht J. and Meijer, H.A.J.
2001 Automatic AMS Sample Combustion and CO_2 Collection, *Radiocarbon* 43, 293–298.

Allen, J.P.
2010 The Second Intermediate Period in the Turin King-List, in: M. Marée (ed.), *The Second Intermediate Period (Thirteenth – Seventeenth Dynasties): Current Research, Future* Prospects, Orientalia Lovaniensia Analecta 192, Leuven, 1–10.

Aston, D.A.
2018 How Early (and How Late) Can Khyan Really Be: An Essay Based on 'Conventional Archaeological Methods', in: I. Forstner-Müller and N. Moeller (eds.), *The Hyksos Ruler Khyan and the Early Second Intermediate Period in Egypt: Problems and Priorities of Current Research*, Vienna, 15–56.

Bietak, M.
1991 Egypt and Canaan during the Middle Bronze Age, *Bulletin of the American Schools of Oriental Research* 281, 27–72.
1997 The Center of Hyksos Rule: Avaris (Tell el-Dabʿa), in: E. Oren (ed.), *The Hyksos: New Historical and Archaeological Perspectives*, Philadelphia, 87–139.
2010 From Where Came the Hyksos and Where Did They Go, in: M. Marée (ed.), *The Second Intermediate Period (Thirteenth – Seventeenth Dynasties): Current Research, Future Prospects*, Orientalia Lovaniensia Analecta 192, Leuven, 139–181.
2015 Recent Discussions about the Chronology of the Middle and the Late Bronze Age in the Eastern Mediterranean: Part I, *Bibliotheca Orientalis* 72, 317–335.
2016 Book Review of Manning, S.W. *A Test of Time and a Test of Time Revisited: The Volcano of Thera and the Chronology and History of the Aegean and East Mediterranean in the Mid-Second Millennium BC.* Oxford, 2014, *Bryn Mawr Classical Review* 2016.04.06. <http://bmcr.brynmawr.edu/2016/2016-04-06.html> (last access 27 July 2019)

Bietak, M., Dorner, J., Hein, I. and Jánosi P.
1994 Neue Grabungsergebnisse aus Tell el-Dabʿa und ʿEzbet Helmi im östlichen Nildelta (1989–1991), *Egypt and the Levant* 4, 9–80.

Bietak, M., Forstner-Müller, I. and Mlinar, C.
2003 The Beginning of the Hyksos Period at Tell el-Dabʿa: A Subtle Change in Material Culture, in: P. Fischer (ed.), *Contributions to the Archaeology and History of the Bronze and Iron Ages in the Eastern Mediterranean: Studies in Honour of Paul Åström*, Vienna, 171–181.

Bietak, M. and Höflmayer, F.
2007 Introduction: High and Low Chronology, in: M. Bietak and E. Czerny (eds.), *The Synchronisation of Civilisations in the Eastern Mediterranean in the Second Millennium B.C. III*, Vienna, 13–23.

Bietak, M., Kopetzky, K., Stager, L.E. and Voss, R.
2008 Synchronisation of Stratigraphies: Ashkelon and Tell el-Dabʿa, *Egypt and the Levant* 18, 49–60.

Braziunas, T.F., Fung, I.E. and Stuiver, M.
1995 The Preindustrial Atmospheric $^{14}CO_2$ Latitudinal Gradient as Related to Exchanges among Atmospheric, Oceanic, and Terrestrial Reservoirs, *Global Biogeochemical Cycles* 9, 565–584.

Bronk Ramsey, C., Dee, M.W., Rowland, J.M., Higham, T.F.G., Harris, S.A., Brock, F., Quiles, A., Wild, E.M. Marcus, E.S. and Shortland, A.J.
2010 Radiocarbon-Based Chronology for Dynastic Egypt, *Science* 328, 1554–1557.

Bruins, H.J.
2007 Charcoal Radiocarbon Dates of Tell el-Dabʿa, in: M. Bietak and E. Czerny (eds.), *The Synchronisation of Civilisations in the Eastern Mediterranean in the Second Millennium B.C. – III*, Vienna, 65–77.
2010 Dating Pharaonic Egypt, *Science* 328 (5985), 1489–1490.

Bruins, H.J. and van der Plicht, J.
2014 The Thera Olive Branch, Akrotiri (Thera) and Palaikastro (Crete): Comparing Radiocarbon Results of the Santorini Eruption, *Antiquity* 88, 282–287.
2017 The Minoan Santorini Eruption and Its ^{14}C Position in Archaeological Strata: Preliminary Comparison between Ashkelon and Tell el Dabʿa, *Radiocarbon* 59.5, 1295–1307.

Cherubini, P., Humbel, T., Beeckman, H., Gärtner, H., Mannes, D., Pearson, C., Schoch, W., Tognetti, R. and Lev-Yadun, S.
2014 The Olive-Branch Dating of the Santorini Eruption, *Antiquity* 88, 267–273.

Dee, M.W., Brock, F., Harris, S.A., Bronk Ramsey, C., Shortland, A.J., Higham, T.F.G. and Rowland, J.M.
2010 Investigating the Likelihood of a Reservoir Offset in the Radiocarbon Record for Ancient Egypt, *Journal of Archaeological Science* 37, 687–693.

Ehrlich, Y., Regev, L. and Boaretto, E.
2018 Radiocarbon Analysis of Modern Olive Wood Raises Doubts concerning a Crucial Piece of Evidence in Dating the Santorini Eruption, *Scientific Reports* 8, 11841, DOI:10.1038/s41598-018-29392-9.

Friedrich, W.L. and Heinemeier, J.
2009 The Minoan Eruption of Santorini Radiocarbon dated to 1613 ± 13 BC, in: Warburton (ed.) 2009, 56–63.

Friedrich, W.L., Kromer, B., Friedrich, M., Heinemeier, J., Pfeiffer, T. and Talamo, S.
2006 Santorini Eruption Radiocarbon Dated to 1627–1600 B.C., *Science* 312, 548.
2014 The Olive Branch Chronology Stands Irrespective of Tree-Ring Counting, *Antiquity* 88, 274–277.

Hagens, G.
2014 Radiocarbon Chronology for Dynastic Egypt and the Tell el-Dabʿa Debate: A Regional Hypothesis, *Egypt and the Levant* 24, 173–190.

Höflmayer, F.
2012 The Date of the Minoan Santorini Eruption: Quantifying the Offset, *Radiocarbon* 54, 435–448.

2017 A Radiocarbon Chronology for the Middle Bronze Age Southern Levant, *Journal of Ancient Egyptian Interconnections* 13, 20–33.

2018 An Early Date for Khyan and Its Implications for Eastern Mediterranean Chronologies, in: I. Forstner-Müller and N. Moeller (eds.), *The Hyksos Ruler Khyan and the Early Second Intermediate Period in Egypt: Problems and Priorities of Current Research*, Vienna, 143–171.

Kutschera, W., Bietak, M., Wild, E.M., Bronk Ramsey, C., Dee, M., Golser, R., Kopetzky, K., Stadler, P., Steier, P., Thanheiser, U. and Weninger, F.

2012 The Chronology of Tell el-Dabʿa: A Crucial Meeting Point of ^{14}C Dating, Archaeology, and Egyptology in the 2nd Millennium BC, *Radiocarbon* 54, 407–422.

Longin, R.

1971 New Method of Collagen Extraction for Radiocarbon Dating, *Nature* 230, 241–242.

Manning, S.W.

2014 *A Test of Time and a Test of Time Revisited*: *The Volcano of Thera and the Chronology and History of the Aegean and East Mediterranean in the Mid-Second Millennium BC,* Oxford.

Manning, S.W., Höflmayer, F., Moeller, N., Dee, M.W., Bronk Ramsey, C., Fleitmann, D., Higham, T.F.G., Kutschera, W. and Wild, E.M.

2014 Dating the Thera (Santorini) Eruption: Coherent Archaeological and Scientific Evidence Supporting a High Chronology, *Antiquity* 88, 1164–1179.

Manning, S.W., Griggs, C., Lorentzen, B., Bronk Ramsey, C., Chivall, D., Jull, A.J.T. and Lange, T.E.

2018 Fluctuating Radiocarbon Offsets Observed in the Southern Levant and Implications for Archaeological Chronology, *Proceedings of the National Academy of Sciences*, <www.pnas.org/cgi/doi/10.1073/pnas.1719420115 > (last access 27 July 2019)

Mook, W.G. and Streurman, H.J.

1983 Physical and Chemical Aspects of Radiocarbon Dating, in: W.G. Mook and H.T. Waterbolk (eds.), *Proceedings of the First International Symposium on ^{14}C and Archaeology, Groningen*, PACT 8, Strasbourg, 31–55.

Pearson, C.L., Brewer, P.W., Brown, D., Heaton, T.J., Hodgins, G.W.L., Jull, A.J.T., Lange, T. and Salzer, M.W.

2018 Annual Radiocarbon Record Indicates 16th Century BCE Date for the Thera Eruption, *Science Advances* 4.8, eaar8241, DOI: 10.1126/sciadv.aar8241.

Van der Plicht, J., Wijma, S., Aerts, A.T., Pertuisot, M.H. and Meijer, H.A.J.

2000 The Groningen AMS Facility: Status Report, *Nuclear Instruments and Methods* B172, 58–65.

Quarta, G., D'Elia, M., Valzano D. and Calcagnile, L.

2005 New Bomb Pulse Radiocarbon Records from Annual Tree Rings in the Northern Hemisphere Temperate Region, *Radiocarbon* 47, 27–30.

Reimer, P.J., Bard, E., Bayliss, A., Beck, J.W., Blackwell, P.G., Bronk Ramsey, C., Buck, C.E., Cheng, H., Edwards, R.L., Friedrich, M., Grootes, P.M., Guilderson, T.P., Haflidason, H., Hajdas, I., Hatté, C., Heaton, T.J., Hoffman, D.L., Hogg, A.Q., Hughen, K.A., Kaiser, K.F., Kromer, B., Manning, S.W., Niu, M., Reimer, R.W., Richards, D.A., Scott, E.M., Southon, J.R., Staff, R.A., Turney, C.S.M. and van der Plicht, J.

2013 IntCal13 and Marine 13 Radiocarbon Age Calibration Curves 0–50,000 Years Cal BP, *Radiocarbon* 55.4, 1869–1887.

Reimer, P.J. et al. (in preparation).

2019 IntCal 19 (title details not yet known), *Radiocarbon* (forthcoming).

Ryholt, K.S.B.

1997 *The Political Situation in Egypt during the Second Intermediate Period, c. 1800–1550 B.C.*, Copenhagen.

Stager, L.E.

2018 Introduction: Ashkelon in the Middle Bronze Age, in: L.E. Stager, J.D. Schloen and R.J. Voss (eds.), *Ashkelon 6: The Middle Bronze Age Ramparts and Gates of the North Slope and Later Fortifications*, Winona Lake, IN, 3–23.

Stager, L.E. and Schloen, J.D.

2008 Introduction: Ashkelon and Its Inhabitants, in: L.E. Stager, J.D. Schloen and D.M. Master (eds.), *Ashkelon 1: Introduction and Overview (1985–2006)*, Winona Lake, IN, 3–10.

Stager, L.E., Schloen, J.D. and Master, D.M. (eds.)

2008 *Ashkelon 1: Introduction and Overview (1985–2006)*, Winona Lake, IN.

Stager, L.E., Schloen, J.D., Master, D.M., Press, M.D. and Aja, A.

2008 Part Four: Stratigraphic Overview, in: L.E. Stager, J.D. Schloen and D.M. Master (eds.), *Ashkelon 1: Introduction and Overview (1985–2006)*, Winona Lake, IN, 213–323.

Synal, H.A., Stocker, M. and Suter, M.

2007 MICADAS: A New Compact Radiocarbon AMS System, *Nuclear Instruments and Methods* B259, 7–13.

Voss, R.J. and Stager, L.E.

2018 The North Tel of Ashkelon in the Bronze and Iron Ages, in: L.E. Stager, J.D. Schloen and R.J. Voss (eds.), *Ashkelon 6: The Middle Bronze Age Ramparts and Gates of the North Slope and Later Fortifications*, Winona Lake, IN, 24–103.

Warburton, D.A. (ed.)

2009 *Time's Up! Dating the Minoan Eruption of Santorini: Acts of the Minoan Eruption Chronology Workshop, Sandbjerg, November 2007,* Aarhus.

Wiener, M.H.

2009 The State of the Debate about the Date of the Theran Eruption, in: Warburton (ed.) 2009, 197–206.

2012 Problems in the Measurement, Calibration, Analysis, and Communication of Radiocarbon Dates (with Special Reference to the Prehistory of the Aegean World), *Radiocarbon* 54.3–4, 423–434.